

# Malaysian brown macroalga *Padina australis* mitigates lipopolysaccharide-stimulated neuroinflammation in BV2 microglial cells

Kogilavani Subermaniam<sup>1,2</sup>, Sze Yuen Lew<sup>1</sup>, Yoon Yen Yow<sup>3</sup>, Siew Huah Lim<sup>4</sup>, Wing Shan Yu<sup>5</sup>, Lee Wei Lim<sup>5</sup>, Kah Hui Wong<sup>1,5\*</sup>

<sup>1</sup> Department of Anatomy, Faculty of Medicine, Universiti Malaya, 50603 Kuala Lumpur, Malaysia

<sup>2</sup> Sungai Buloh Training Institute of Ministry of Health Malaysia, Jalan Hospital, 47000 Sungai Buloh, Selangor, Malaysia

<sup>3</sup> Department of Biological Sciences, School of Medical and Life Sciences, Sunway University, 47500 Bandar Sunway, Selangor Darul Ehsan, Malaysia

<sup>4</sup> Department of Chemistry, Faculty of Science, Universiti Malaya, 50603 Kuala Lumpur, Malaysia

<sup>5</sup> Neuromodulation Laboratory, School of Biomedical Sciences, Li Ka Shing Faculty of Medicine, The University of Hong Kong, 21 Sassoon Road, Pokfulam, Hong Kong Special Administrative Region, China

## ARTICLE INFO

**Article type:**  
Original

**Article history:**  
Received: Sep 12, 2022  
Accepted: Mar 6, 2023

**Keywords:**  
Brown algae  
BV2 microglial  
Cytokines  
Major compounds  
Neuroinflammation  
Oxidative damage

## ABSTRACT

**Objective(s):** Neuroinflammation and microglial activation are pathological features in central nervous system disorders. Excess levels of reactive oxygen species (ROS) and pro-inflammatory cytokines have been implicated in exacerbation of neuronal damage during chronic activation of microglial cells. *Padina australis*, a brown macroalga, has been demonstrated to have various pharmacological properties such as anti-neuroinflammatory activity. However, the underlying mechanism mediating the anti-neuroinflammatory potential of *P. australis* remains poorly understood. We explored the use of Malaysian *P. australis* in attenuating lipopolysaccharide (LPS)-stimulated neuroinflammation in BV2 microglial cells.

**Materials and Methods:** Fresh specimens of *P. australis* were freeze-dried and subjected to ethanol extraction. The ethanol extract (PAEE) was evaluated for its protective effects against 1 µg/ml LPS-stimulated neuroinflammation in BV2 microglial cells.

**Results:** LPS reduced the viability of BV2 microglia cells and increased the levels of nitric oxide (NO), prostaglandin E<sub>2</sub> (PGE<sub>2</sub>), intracellular reactive oxygen species (ROS), inducible nitric oxide synthase (iNOS), cyclooxygenase-2 (COX-2), tumor necrosis factor-alpha (TNF-α), and interleukin-6 (IL-6). However, the neuroinflammatory response was reversed by 0.5–2.0 mg/ml PAEE in a dose-dependent manner. Analysis of liquid chromatography-mass spectrometry (LC-MS) of PAEE subfractions revealed five compounds; methyl α-eleostearate, ethyl α-eleostearate, niacinamide, stearamide, and linoleic acid.

**Conclusion:** The protective effects of PAEE against LPS-stimulated neuroinflammation in BV2 microglial cells were found to be mediated by the suppression of excess levels of intracellular ROS and pro-inflammatory mediators and cytokines, denoting the protective role of *P. australis* in combating continuous neuroinflammation. Our findings support the use of *P. australis* as a possible therapeutic for neuroinflammatory and neurodegenerative diseases.

► Please cite this article as:

Subermaniam K, Lew SY, Yow YY, Lim SH, Yu WS, Lim LW, Wong KH. Malaysian brown macroalga *Padina australis* mitigates lipopolysaccharide-stimulated neuroinflammation in BV2 microglial cells. Iran J Basic Med Sci 2023; 26: 669-679. doi: <https://dx.doi.org/10.22038/IJBMS.2023.67835.14842>

## Introduction

Emerging evidence suggests that neuroinflammation plays an important role in the onset and progression of neurodegenerative diseases. The neuroinflammatory response is mediated by cytokines, chemokines, reactive oxygen species (ROS), and secondary messengers produced by microglia, astrocytes, endothelial cells, peripherally derived T cells, macrophages, and dendritic cells, leading to physiological, biochemical, and psychological consequences (1). Microglia are the resident macrophages of the central nervous system (CNS) and make up approximately 5% to 12% of the total cell population in the CNS. Microglia have been observed to colonize the brain as early as embryonic day 9.5 (E9.5) of development before the emergence of neurons and other glia, and subsequently proliferate and persist throughout one's lifetime (2). During development,

microglia play an active phagocytic role in mediating synaptic pruning and neuronal circuit formation (3). Chronic microglial activation can be triggered by either a single pathogenic stimulus or exposure to multiple stimuli, resulting in cumulative neuronal loss over time. In CNS diseases, reactive microgliosis and ROS have been found to exacerbate the chronic deleterious activation of microglial (4).

Lipopolysaccharide (LPS) is an endotoxin derived from the outer membrane of Gram-negative bacteria. It is primarily recognized by the CD14/Toll-like receptor 4 (TLR-4) receptor complex, which is expressed on microglia and astrocytes. TLR-4 signaling mediates autoimmune responses and neuroinflammation in neurodegenerative diseases (5). Activated microglia generate massive amounts of ROS, acquire a pro-inflammatory cellular profile, and release pro-inflammatory cytokines. Indeed, chronic

neuroinflammation involves long-standing activation of microglia and subsequent sustained release of inflammatory mediators resulting in increased oxidative and nitrosative damage (6).

Marine algae are rich in secondary metabolites with therapeutic potential, including phlorotannins, alginates, fucoidan, sargaquinoic acid, sulfated polysaccharides, and carotenoids, which are not commonly found in terrestrial plants (7-11). One such seaweed is brown macroalga, *Padina australis* Hauck 1887 (Figure 1), which can be found in the *slow-moving* and shallow waters across the tropical and subtropical regions. Brown macroalgae play an essential role in coastal ecosystems including acting as structures, trapping nutrients and carbon, producing oxygen, and generating biomass (12-15). *P. australis* can be found in lower intertidal to deep subtidal zones along the moderately wave-exposed shorelines of coastal regions. It can be spotted *anchored* to a solid *substrate* by a discoid holdfast on coral rubble, reef flats, tidepools, and fishing nets (16). *P. australis* possesses pharmacological properties such as anti-oxidant (17-19), anti-neuroinflammatory (17), antimicrobial (20, 21), antiacetylcholinesterase (17, 18), anticancer (22), antiviral (23), antiangiogenic (24), and neurotrophic (25) activity. Our recent findings showed that *P. australis* promoted antidepressant-like effects in an *in vitro* model, suggesting its potential development as a mitochondria-targeted anti-oxidant (16).

However, the mechanism of the anti-neuroinflammatory activity of *P. australis* remains elusive. In this study, we investigated the anti-neuroinflammatory properties of *P. australis* ethanol extract (PAEE) on the regulation of pro-inflammatory mediators (nitric oxide, NO; prostaglandin E<sub>2</sub>, PGE<sub>2</sub>; inducible nitric oxide synthase, iNOS; and cyclooxygenase-2, COX-2) and pro-inflammatory cytokines (interleukin-6, IL-6 and tumor necrosis factor  $\alpha$ , TNF- $\alpha$ ) in LPS-stimulated BV2 microglial cells.

## Materials and Methods

### Harvesting of *P. australis* and preparation of the ethanol extract

Fresh specimens of *P. australis* were harvested from Cape Rachado located in Negeri Sembilan, West Coast of Peninsular Malaysia. Morphological identification was conducted using standard botanical approaches (26). Specimens were washed with salt water, freeze-dried (LaboGene, Brigachtal) for 48 to 72 hr at  $-50\pm 2$  °C, and ground into a fine powder (16). Solvent extraction was conducted using the sequential maceration method with extractants of increasing polarity. The ethanol extract (PAEE) was then concentrated *in vacuo* (LaboGene, Brigachtal), dissolved in Minimum Essential Medium Eagle (MEM) (Sigma-Aldrich, St. Louis, MO, USA, USA), and filtered-sterilized through a 0.2  $\mu$ m-rated nylon membrane filter (16).

### BV2 microglial cell culture

The BV2 murine microglial cell line (Elabscience Biotechnology, Wuhan, Hubei, China) is an immortalized cell line that demonstrates the functional and morphological characteristics of microglia. BV2 microglial cells were maintained in Minimum Essential Medium Eagle (MEM) (Sigma-Aldrich, St. Louis, MO, USA, USA) supplemented with 10% (v/v) fetal bovine serum and 1% (v/v) penicillin-streptomycin at  $37\pm 2$  °C in a 5% CO<sub>2</sub>-humidified incubator.

BV2 cells without any treatment served as a negative control, whereas cells treated with 250  $\mu$ M N $\omega$ -Nitro-L-arginine methyl ester (L-NAME) (Sigma-Aldrich, St. Louis, MO, USA, USA) served as a positive control (27).

### 3-(4,5-Dimethylthiazol-2-yl)-2,5-diphenyltetrazolium bromide (MTT) cell viability assay

The BV2 cells were plated into a 96-well plate at a density of  $6.25 \times 10^4$  cells per well and incubated for 24 hr at  $37\pm 2$  °C in a 5% CO<sub>2</sub>-humidified incubator. The supernatant was discarded and replaced with fresh medium containing different concentrations of selected PAEE (0.25–8.0 mg/ml) (16) and incubated for 24 hr (designated as Experiment 2.3A) or different concentrations of LPS (0.125–8.0  $\mu$ g/ml) (*Escherichia coli* O55: B5, L4524 Sigma-Aldrich, St. Louis, MO, USA) and incubated for 24 hr (designated as Experiment 2.3B).

The protective effects of PAEE against LPS-stimulated cytotoxicity in BV2 cells were studied by pre-treating the cells with a selected range of concentrations from Experiment 2.3A (0.25–2.0 mg/ml) for 2 hr followed by 1  $\mu$ g/ml LPS for 24 hr (designated as Experiment 2.3C). Ten microliter of 0.5 mg/ml MTT (Merck & Co, Rahway, NJ) was added to each well and incubated for 4 hr. Supernatant was discarded, and insoluble formazan was dissolved in 100  $\mu$ l dimethyl sulfoxide (DMSO). The MTT reduction was determined spectrophotometrically at 570 nm with a reference wavelength of 630 nm in a UV-Vis spectrophotometer microplate reader (Infinite 200 Pro, Männedorf, Switzerland) and expressed as a percentage of viable cells relative to the negative control.

The most optimum concentration of PAEE determined based on Experiment 2.3C (0.25–2.0 mg/ml) and 1  $\mu$ g/ml LPS were selected for subsequent assays of neuroinflammation.

### Measurement of nitric oxide production

The production of NO was measured according to the method described by Oh *et al.* (28) with minor modifications. The BV2 cells were plated into a 96-well plate at a density of  $6.25 \times 10^4$  cells per well and incubated for 24 hr at  $37\pm 2$  °C in a 5% CO<sub>2</sub>-humidified incubator. The supernatant was discarded and pre-treated with fresh medium containing 0.25, 0.5, 1.0, or 2.0 mg/ml PAEE or 250  $\mu$ M L-NAME for 2 hr before exposure to 1  $\mu$ g/ml LPS for 24 hr. A total of 100  $\mu$ l supernatant was transferred to a 96-well plate, to which was added the same volume of Griess reagent (1% [w/v] sulfanilamide and 0.1% [w/v] N-1-naphthylethylenediamine



**Figure 1.** An underwater view of *Padina australis* Hauck, 1887 at Cape Rachado, Port Dickson, Negeri Sembilan, Malaysia

dihydrochloride in 5% [v/v] phosphoric acid; Cell Signaling Technology, Danvers, MA, USA). The NO production was determined spectrophotometrically at 550 nm in a UV-Vis spectrophotometer microplate reader (Infinite 200 Pro, Männedorf, Switzerland) and expressed as micromolar ( $\mu\text{M}$ ) relative to the negative control.

#### Measurement of prostaglandin $E_2$ production

The BV2 microglial cells were plated into a 96-well plate at a density of  $6.25 \times 10^4$  cells per well and incubated for 24 hr at  $37 \pm 2$  °C in a 5%  $\text{CO}_2$ -humidified incubator. The supernatant was discarded and pre-treated with fresh medium containing 0.5, 1.0, or 2.0 mg/ml PAEE for 2 hr before exposure to 1  $\mu\text{g}/\text{ml}$  LPS for 24 hr. The supernatant was then subjected to  $\text{PGE}_2$  measurement by enzyme-linked immunosorbent assay (ELISA) according to the manufacturer's protocol of Parameter™ Prostaglandin  $E_2$  Immunoassay (R&D Systems, Minneapolis, MN). The  $\text{PGE}_2$  production was determined spectrophotometrically at 450 nm with a reference wavelength of 570 nm in a UV-Vis spectrophotometer microplate reader (Infinite 200 Pro, Männedorf, Switzerland) and expressed as picogram per milliliter (pg/ml) relative to the negative control.

#### Intracellular reactive oxygen species assay

The intracellular ROS level was determined according to protocols described by Subermaniam *et al.* (16) with minor modifications. The BV2 microglial cells were plated into a 96-well plate at a density of  $6.25 \times 10^4$  cells per well and incubated for 24 hr at  $37 \pm 2$  °C in a 5%  $\text{CO}_2$ -humidified incubator. The supernatant was discarded and pre-treated with fresh medium containing 0.5, 1.0, or 2.0 mg/ml PAEE for 2 hr before exposure to 1  $\mu\text{g}/\text{ml}$  LPS for 24 hr. The supernatant was removed and replaced with 25  $\mu\text{M}$  of 2',7'-dichlorofluorescein diacetate (DCFH-DA) (Sigma-Aldrich, St. Louis, MO, USA), further incubated for 30 min at  $37 \pm 2$  °C, and washed twice with phosphate buffer saline (PBS). The fluorescence intensity was determined spectrophotometrically at an excitation wavelength of 485 nm and emission wavelength of 535 nm in a UV-Vis spectrophotometer microplate reader (Infinite 200 Pro, Männedorf, Switzerland) and expressed as a percentage relative to the negative control.

#### Western blot analysis

Western blot analysis was carried out according to the method described by Kim *et al.* (29) with minor modifications. The BV2 microglial cells were plated into a 96-well plate at a density of  $6.25 \times 10^4$  cells per well and incubated for 24 hr at  $37 \pm 2$  °C in a 5%  $\text{CO}_2$ -humidified incubator. The supernatant was discarded and pre-treated with fresh medium containing 0.5, 1.0, or 2.0 mg/ml PAEE for 2 hr before exposure to 1  $\mu\text{g}/\text{ml}$  LPS for 24 hr. The lysate was diluted in lysis buffer containing protease inhibitor cocktail (Sigma-Aldrich, St. Louis, MO, USA) and 1 mM phenylmethylsulfonyl fluoride (Calbiochem, San Diego, CA, USA). An equal amount of proteins (20  $\mu\text{g}$ ) was separated in 10% sodium dodecyl sulfate-polyacrylamide gel electrophoresis (SDS-PAGE) and transferred to polyvinylidene fluoride (PVDF) membranes (Amersham Biosciences, Piscataway, NJ, USA). The membranes were blocked with 5% skim milk in TBST (Tris-buffered saline in 0.1% TWEEN® 20) buffer for 1 hr at room temperature and incubated with primary antibodies [rabbit (mouse-

specific) monoclonal anti-iNOS antibody, Cat. No. 13120, 1:1000 dilution, or rabbit (mouse-specific) monoclonal anti-COX-2 antibody, Cat. No. 12282, 1:1000 dilution, Cell Signaling Technology, Danvers, MA, USA] in blocking buffer at 4 °C overnight in a humidity chamber.

After washing five times in TBST, the membranes were incubated with a secondary antibody (horseradish peroxidase (HRP)-conjugated) for 1 hr at room temperature. Proliferating cell nuclear antigen (PCNA; Cell Signaling Technology, Danvers, MA, USA) and  $\beta$ -actin (Cell Signaling Technology, Danvers, MA, USA) were employed as the loading controls. The HRP signal was detected by chemiluminescence (WesternBright™ ECL Spray, Advansta Inc, San Jose, CA, USA) and visualized using the LAS-3000 LuminoImage analyzer (Fujifilm, Tokyo, Japan). Resultant bands were quantified with Image J densitometry (National Institutes of Health and the Laboratory for Optical and Computational Instrumentation, Madison, WI, USA) and normalized to  $\beta$ -actin (rabbit monoclonal antibody, Cat. No. 4970, 1:1000, Cell Signaling Technology, Danvers, MA, USA).

#### Measurement of pro-inflammatory cytokine secretion

The BV2 microglial cells were plated into a 96-well plate at a density of  $6.25 \times 10^5$  cells per well and incubated for 24 hr at  $37 \pm 2$  °C in a 5%  $\text{CO}_2$ -humidified incubator. The supernatant was discarded and pre-treated with fresh medium containing 0.5, 1.0, or 2.0 mg/ml PAEE for 2 hr before exposure to 1  $\mu\text{g}/\text{ml}$  LPS for 24 hr. The supernatant was collected, and the production of TNF- $\alpha$  and IL-6 was measured using the Mouse TNF- $\alpha$  Quantikine ELISA Kit and Mouse IL-6 Quantikine ELISA Kit (R&D Systems, Minneapolis, MN, USA). The concentration of TNF- $\alpha$  or IL-6 was determined by measuring the absorbance at 450 nm and 570 nm as reference wavelengths in a UV-Vis spectrophotometer microplate reader and expressed as picogram per milliliter (pg/ml) relative to the negative control.

#### Isolation and identification of compounds from PAEE

PAEE was subjected to flash column chromatography (Silica gel 60, 0.04-0.06 mm; Merck, Darmstadt, Germany). The polarity of the eluting solvent was gradually increased starting from chloroform:hexanes (1:1) to chloroform:methanol (99:1-85:15). Eluted fractions were monitored via thin-layer chromatography (TLC) and appropriate fractions were combined into 11 main fractions (A-K). The selected combined fractions (C, F, and K) were further fractionated using preparative radial chromatography (PRC) (Silica gel 60 PF<sub>254</sub>, Merck, Darmstadt, Germany) into five, nine, and seven subfractions, respectively. The solvent systems used in the PRC included chloroform:hexanes (1-2:1-3), diethyl ether:hexanes (3:1), and dichloromethane. The eluted subfractions (1<sup>st</sup>, 9<sup>th</sup>, and 2<sup>nd</sup> subfractions from fractions C, F, and K, respectively) were concentrated and further analyzed by liquid chromatography-mass spectrometry (LC-MS). Figure 2 shows the workflow of the extraction process and fractionation of *P. australis*.

The LC-MS analysis was performed on Agilent 1290 infinity liquid chromatograph (Agilent Technologies, Wilmington, DE, USA), coupled to the Agilent 6520 Accurate-Mass Q-TOF mass spectrometer with dual electrospray ionization (ESI) source. A reverse-phase high-performance liquid chromatography (HPLC) column

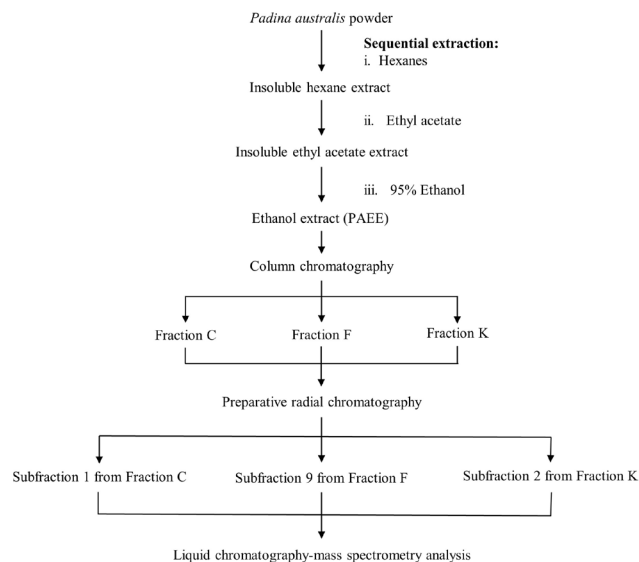


**Figure 2.** Extraction process and fractionation of *Padina australis*

(Agilent Eclipse XBD-C18) with a length of 150 mm and an internal diameter of 2.1 mm in a narrow-bore scale format along with a particle size of 3.5  $\mu\text{m}$  was used (30). Automated mass spectrometry - mass spectrometry (aMSMS) mode was employed. Data were processed using Agilent MassHunter Qualitative Analysis software (Version B.07.00) and the Molecular Feature Extraction (MFE) small molecule algorithm. Compound identification was performed using the MassHunter METLIN Metabolite Personal Compound Database and Library (PCDL) (Agilent Technologies, Santa Clara, CA, USA).

### Statistical analysis

Data analysis was performed using the Statistical Package for Social Sciences (SPSS, version 23.0 for Windows, Chicago, IL, USA). Data were expressed as mean  $\pm$  standard deviation (SD) from three replicates. The distribution of variables (assumptions of normality) was determined using the Shapiro-Wilk test whereas Levene's test was employed to assess the homogeneity of variance. For normally distributed data, one-way ANOVA followed by Bonferroni *post hoc* multiple comparison tests were used for equal variances assumed, whereas the Welch test followed by Games-Howell multiple comparison test were used for equal variances not assumed. For non-normally distributed data, Kruskal-Wallis one-way ANOVA (k samples) followed by pairwise multiple comparison test were used. A *P*-value of  $<0.05$  was considered statistically significant.

## Results

### Effect of PAEE on the viability of BV2 microglial cells

The effect of PAEE on the viability of BV2 microglial cells was evaluated preceding the investigation of the anti-neuroinflammatory activities of the extract to eliminate the possible cytotoxic and proliferative effects. As shown in Figure 3a, cell viability was decreased with increasing concentrations of PAEE from 1.0 to 2.0 mg/ml, but was markedly reduced at 4.0 and 8.0 mg/ml in which the viability was significantly decreased to  $23.79 \pm 4.72$  and  $10.47 \pm 0.43\%$ , respectively compared with the negative control ( $P < 0.05$ ). Considering the lower concentrations of 0.25 to 2.0 mg/ml PAEE showed no significant difference in viability compared with the negative

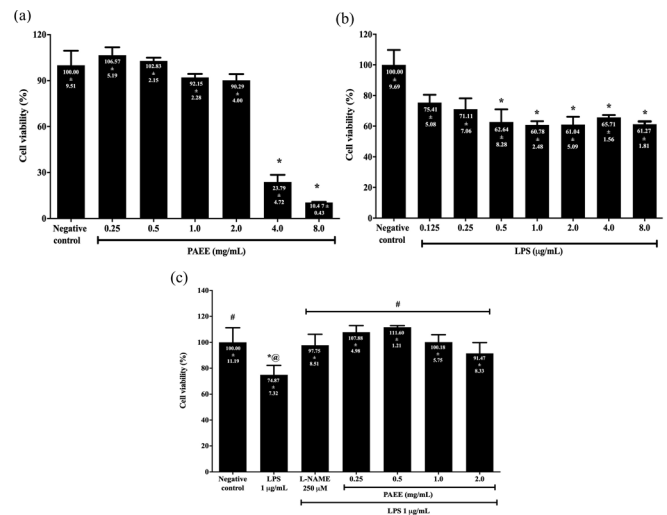


**Figure 3.** Effect of (a) PAEE and (b) LPS on the viability of BV2 microglial cells following incubation with different concentrations of PAEE and LPS for 24 hr. Asterisk (\*) denotes significant difference ( $P < 0.05$ ; using Games Howell for PAEE and Kruskal-Wallis for LPS) in viability relative to the negative control. (c) Effect of PAEE on the viability of BV2 microglial cells following pretreatment with different concentrations of ethanol extract for 2 hr and exposure to 1  $\mu\text{g/ml}$  of LPS for 24 hr. Asterisk (\*), hash (#), and alias (@) denote a significant difference ( $P < 0.05$ ; Bonferroni) in viability relative to the negative control, LPS, and L-NAME, respectively. L-NAME: N $\omega$ -Nitro-L-arginine methyl ester; LPS: Lipopolisaccharide; PAEE: *Padina australis* ethanol extract

control ( $P > 0.05$ ), the concentration range was selected for subsequent assays of viability and NO production.

### Effect of LPS on the viability of BV2 microglial cells

The vulnerability of BV2 microglial cells to LPS-stimulated toxicity was investigated through exposure to different concentrations of LPS in the range of 0.125 to 8.0  $\mu\text{g/ml}$ . Figure 3b shows that cell viability was decreased with increasing LPS concentrations. At 0.5, 1.0, 2.0, 4.0, and 8.0  $\mu\text{g/ml}$  LPS, the viability was significantly decreased to  $62.64 \pm 8.28$ ,  $60.78 \pm 2.48$ ,  $61.04 \pm 5.09$ ,  $65.71 \pm 1.56$ , and  $61.27 \pm 1.81\%$ , respectively ( $P < 0.05$ ). Considering exposure to 1  $\mu\text{g/ml}$  LPS caused the lowest percentage of viability at  $60.78 \pm 2.48$ , the concentration was selected for the subsequent assays of neuroinflammation.

### Effect of PAEE on the viability of BV2 microglial cells treated with LPS

The protective effect of PAEE against 1  $\mu\text{g/ml}$  LPS-stimulated cytotoxicity was investigated by pretreating BV2 microglial cells with 0.25 to 2.0 mg/ml PAEE for 2 hr followed by 1  $\mu\text{g/ml}$  LPS for 24 hr. As shown in Figure 3c, 1  $\mu\text{g/ml}$  LPS significantly reduced the viability to  $74.87 \pm 7.32\%$  or 1.3-fold lower compared with the negative control ( $P < 0.05$ ). However, pretreatment with PAEE in the range of 0.25 to 2.0 mg/ml and L-NAME significantly increased the viability to  $107.88 \pm 4.98\%$  (0.25 mg/ml),  $111.60 \pm 1.21\%$  (0.5 mg/ml),  $100.18 \pm 5.75\%$  (1.0 mg/ml),  $91.47 \pm 8.33\%$  (2.0 mg/ml), and  $97.75 \pm 8.51\%$  (L-NAME) or 1.2- to 1.5-fold higher compared with LPS ( $P < 0.05$ ). We did not observe cytotoxicity effect for any tested concentrations (0.25 to 2.0 mg/ml) ( $P > 0.05$ ). Pre-treatment with PAEE was observed to be comparable with the effect of L-NAME in increasing viability.

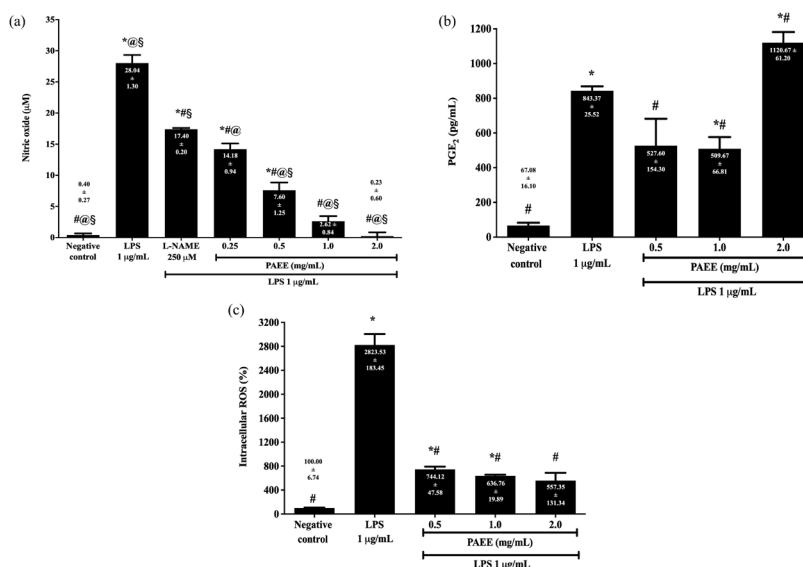


**Figure 4.** Effect of PAEE on (a) NO and (b) PGE<sub>2</sub> production, and (c) intracellular ROS generation in BV2 microglial cells following pretreatment with different concentrations of PAEE for 2 hr and exposure to 1 µg/ml of LPS for 24 hr. Asterisk (\*), hash (#), alias (@), and section (§) denote a significant difference [ $P < 0.05$ ; Bonferroni (NO) and Games-Howell (PGE<sub>2</sub> and intracellular ROS)] in NO and PGE<sub>2</sub> production, and intracellular ROS level relative to the negative control, LPS, L-NAME, and 0.25 mg/ml PAEE, respectively  
L-NAME: Nω-Nitro-L-arginine methyl ester; LPS: Lipopolysaccharide; NO: Nitric oxide; PAEE: *Padina australis* ethanol extract; PGE<sub>2</sub>: Prostaglandin E<sub>2</sub>; ROS: Reactive oxygen species

**Effect of PAEE on NO production in BV2 microglial cells treated with LPS**

We evaluated NO production in culture supernatants by detecting the level of nitrite using a Griess reaction. As shown in Figure 4a, 1 µg/ml LPS significantly increased the NO production from 0.40 ± 0.27 µM to 28.04 ± 1.30 µM or 70.1-fold higher compared with the negative control ( $P < 0.05$ ). However, pretreatment with PAEE in the range of 0.25 to 2.0 mg/ml and L-NAME significantly reduced NO production to 14.18 ± 0.94 µM (0.25 mg/ml), 7.60 ± 1.25 µM (0.5 mg/ml), 2.62 ± 0.84 µM (1.0 mg/ml), 0.23 ± 0.60 µM (2.0 mg/ml), and 17.40 ± 0.20 µM (L-NAME) or 1.6- to 121.9-fold lower compared with LPS ( $P < 0.05$ ).

Although 0.25 mg/ml PAEE suppressed NO production to 14.18 ± 0.94 µM or 2.0-fold lower compared with LPS, it exhibited a weaker inhibitory effect against NO production

compared with 0.5 to 2.0 mg/ml PAEE ( $P < 0.05$ ). Thus, higher concentrations of PAEE (0.5 to 2.0 mg/ml) were selected for subsequent assays of neuroinflammation. Interestingly, the tested concentrations of PAEE exhibited 1.2- to 75.7-fold higher inhibitory activity compared with L-NAME ( $P < 0.05$ ).

**Effect of PAEE on PGE<sub>2</sub> production in BV2 microglial cells treated with LPS**

COX-2 catalyzes the conversion of free arachidonic acid to prostaglandins in LPS-stimulated neuroinflammation. As shown in Figure 4b, 1 µg/ml LPS significantly increased PGE<sub>2</sub> production from 67.08 ± 16.10 pg/ml to 843.37 ± 25.52 pg/ml or 12.6-fold higher compared with the negative control ( $P < 0.05$ ). However, pretreatment with 0.5 and 1.0 mg/ml PAEE significantly suppressed the PGE<sub>2</sub> production

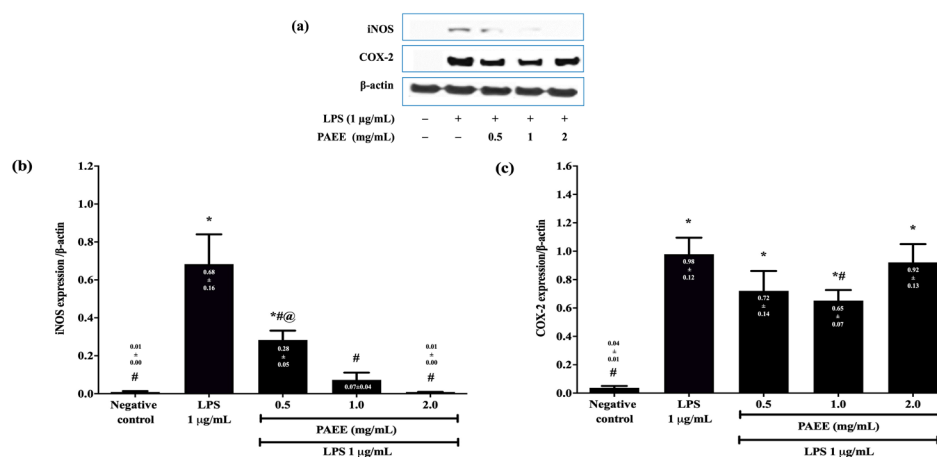


**Figure 5.** Effect of PAEE on the protein expression of iNOS and COX-2 in BV2 microglial cells following pretreatment with different concentrations of PAEE for 2 hr and exposure to 1 µg/ml of LPS for 24 hr. iNOS and COX-2 were evaluated by western blot analysis (a), the relative expression of iNOS (b), and COX-2 (c) were evaluated by densitometry with β-actin as an internal protein control. The bands corresponding to iNOS and COX-2 are noticeably more intense in LPS compared with that of negative control, whereas PAEE showed less intense bands with LPS. Asterisk (\*) and hash (#) denote a significant difference [ $P < 0.05$ ; Games-Howell (iNOS) and Bonferroni (COX-2)] in the expression of iNOS and COX-2 relative to the negative control and LPS, respectively  
COX-2: Cyclooxygenase-2; iNOS: Inducible nitric oxide synthase; LPS: Lipopolysaccharide; PAEE: *Padina australis* ethanol extract

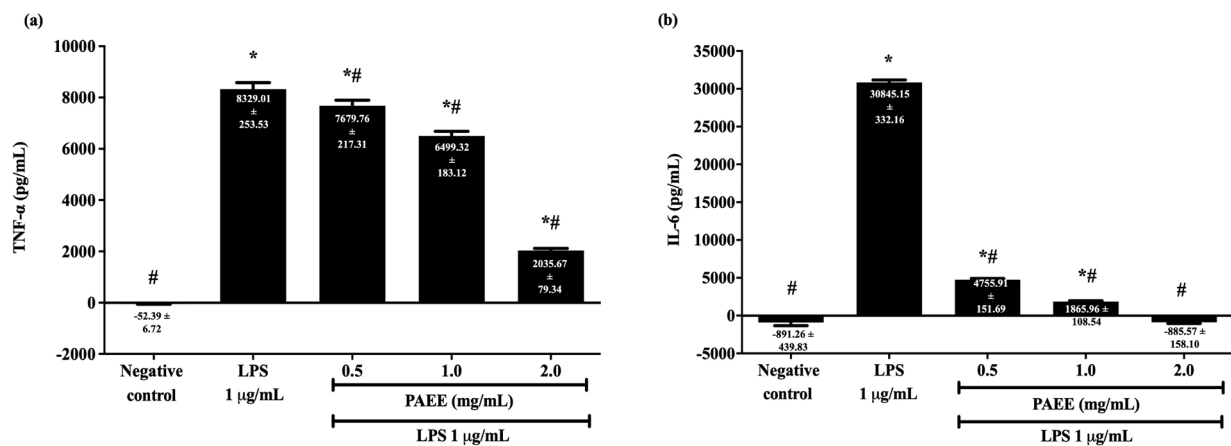


**Figure 6.** Effect of PAEE on the expressions of (a) TNF- $\alpha$  and (b) IL-6 in BV2 microglial cells following pretreatment with different concentrations of PAEE for 2 hr and exposure to 1  $\mu$ g/ml of LPS for 24 hr. Asterisk (\*) and hash (#) denote a significant difference [ $P < 0.05$ ; Bonferroni (TNF- $\alpha$ ) and Games-Howell (IL-6)] in the TNF- $\alpha$  and IL-6 concentrations relative to the negative control and LPS, respectively. IL-6: Interleukin-6; LPS: Lipopolysaccharide; PAEE: *Padina australis* ethanol extract; TNF- $\alpha$ : Tumor necrosis factor- $\alpha$

to 527.60  $\pm$  154.30 and 509.67  $\pm$  66.81 pg/ml or 1.6- and 1.7-fold lower compared with LPS ( $P < 0.05$ ), respectively. On the other hand, 2.0 mg/ml PAEE failed to inhibit PGE<sub>2</sub> production and actually increased PGE<sub>2</sub> levels to 1120.67  $\pm$  61.20 pg/ml or 1.3-fold higher compared with LPS ( $P < 0.05$ ).

#### Effect of PAEE on intracellular ROS generation in BV2 microglial cells treated with LPS

ROS act as second messengers to amplify the inflammatory function of microglia, activate the antioxidant response elements, and restore redox homeostasis. As shown in Figure 4c, 1  $\mu$ g/ml LPS significantly increased the intracellular ROS level from 100.00  $\pm$  6.74% to 2823.53  $\pm$  183.45% or 28.2-fold higher compared with the negative control ( $P < 0.05$ ). However, pretreatment with 0.5, 1.0, and 2.0 mg/ml PAEE significantly reduced ROS generation to 744.12  $\pm$  47.58, 636.76  $\pm$  19.89, and 557.35  $\pm$  131.34% or 3.8- to 5.1-fold lower compared with LPS ( $P < 0.05$ ).

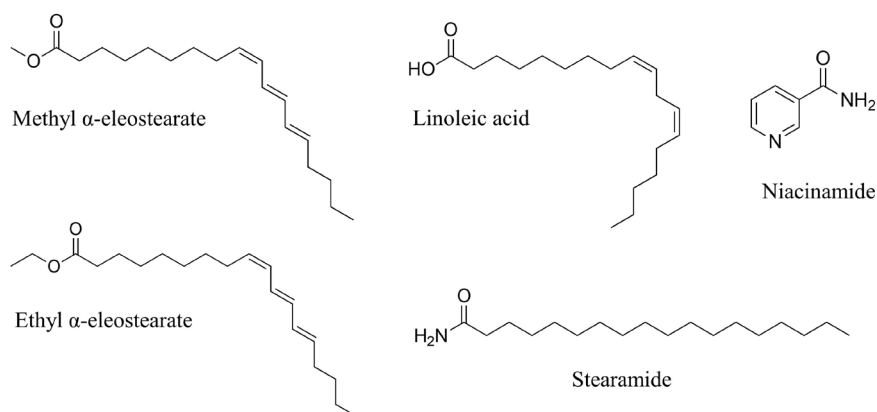
#### Effect of PAEE on the expression of iNOS and COX-2 in BV2 microglial cells treated with LPS

Figure 5a shows the Western blot analysis of iNOS and COX-2 expression. Treatment with 1  $\mu$ g/ml LPS significantly increased the iNOS expression from 0.01  $\pm$  0.00 to 0.68  $\pm$  0.16 or 68.0-fold higher compared with the negative control ( $P < 0.05$ ) (Figure 5b). However, pretreatment with 0.5, 1.0, and 2.0 mg/ml PAEE down-regulated iNOS expression in a dose-dependent manner to 0.28  $\pm$  0.05, 0.07  $\pm$  0.04, and

0.01  $\pm$  0.00 or 2.4-, 9.7-, and 68.0-fold lower compared with LPS ( $P < 0.05$ ), respectively. Treatment with 1  $\mu$ g/ml LPS also significantly increased COX-2 expression from 0.04  $\pm$  0.01 to 0.98  $\pm$  0.12 or 24.5-fold higher compared with the negative control ( $P < 0.05$ ) (Figure 5c). However, only 1.0 mg/ml PAEE significantly reduced COX-2 expression to 0.65  $\pm$  0.07 or 1.5-fold lower compared with LPS ( $P < 0.05$ ).

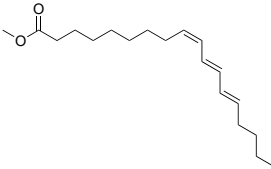
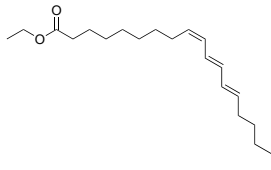
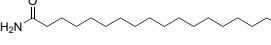
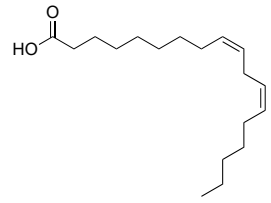
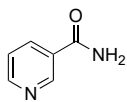
#### Effect of PAEE on the secretion of TNF- $\alpha$ and IL-6 in BV2 microglial cells treated with LPS

Activated BV2 microglial cells showed induced secretion of pro-inflammatory cytokines, including TNF- $\alpha$  and IL-6. As shown in Figure 6a, 1  $\mu$ g/ml of LPS significantly increased the secretion of TNF- $\alpha$  from -52.39  $\pm$  6.72 pg/ml to 8329.01  $\pm$  253.53 pg/ml or 100.63% higher compared with the negative control ( $P < 0.05$ ). However, pretreatment with 0.5, 1.0, and 2.0 mg/ml PAEE suppressed the TNF- $\alpha$  secretion to 7679.76  $\pm$  217.31, 6499.32  $\pm$  183.12, and 2035.67  $\pm$  79.34 pg/ml, or 7.80, 21.97 and 75.56% lower compared with LPS ( $P < 0.05$ ), respectively. As shown in Figure 6b, 1  $\mu$ g/ml of LPS significantly increased the secretion of IL-6 from -891.26  $\pm$  439.83 pg/ml to 30845.15  $\pm$  332.16 pg/ml or 102.89% higher compared with the negative control ( $P < 0.05$ ). However, pretreatment with 0.5, 1.0, and 2.0 mg/ml PAEE markedly suppressed the IL-6 secretion to 4755.91  $\pm$  151.69, 1865.96  $\pm$  108.54, and -885.57  $\pm$  158.10 pg/ml, or 84.58, 93.95 and 102.87% lower compared with LPS ( $P < 0.05$ ), respectively.



**Figure 7.** Identified compounds from *Padina australis* ethanol extract

**Table 1.** Isolated and identified compounds from *Padina australis* ethanol extract based on liquid chromatography mass spectrometry/mass spectrometry (LCMS/MS) analysis

Compound	Molecular structure	Molecular formula	Molecular ion peak ( <i>m/z</i> )
Methyl $\alpha$ -eleostearate (9 <i>Z</i> ,11 <i>E</i> ,13 <i>E</i> -octadecatrienoic acid methyl ester)		C <sub>19</sub> H <sub>32</sub> O <sub>2</sub>	293.2471
Ethyl $\alpha$ -eleostearate (9 <i>Z</i> ,11 <i>E</i> ,13 <i>E</i> -octadecatrienoic acid ethyl ester)		C <sub>20</sub> H <sub>34</sub> O <sub>2</sub>	307.2628
Stearamide (Octadecanamide)		C <sub>18</sub> H <sub>37</sub> NO	284.2953
Linoleic acid (9 <i>Z</i> ,12 <i>Z</i> -octadecadienoic acid)		C <sub>18</sub> H <sub>32</sub> O <sub>2</sub>	281.246
Niacinamide (3-pyridinecarboxamide)		C <sub>6</sub> H <sub>6</sub> N <sub>2</sub> O	123.0531

### Identification of the major compounds in PAEE fractions

Liquid chromatography-mass spectrometry (LC-MS/MS using aMSMS mode) analysis of subfractions C-1, F-9, and K-2 detected 93, 73, and 31 corresponding peaks in the positive ion mass spectra. A total of five major compounds were identified by searching the Metlin database using a molecular formula generator (MFG) mass score above 90% and a mass deviation [difference between observed (*m/z*) and calculated (MFG) mass] of  $\pm 5$  ppm. These compounds included two esters, and an amide (stearamide) (31) from subfraction C-1, a polyunsaturated fatty acid (PUFA) (linoleic acid) from subfraction F-9, and an amide (niacinamide, a major form of vitamin B3) (32) from subfraction K-2 (Figure 7).

The ESIMS of subfraction C-1 shows molecular ion peaks at *m/z* 293.2471, 307.2628, and 307.2628, establishing the molecular formula of methyl  $\alpha$ -eleostearate (C<sub>19</sub>H<sub>32</sub>O<sub>2</sub>), ethyl  $\alpha$ -eleostearate (C<sub>20</sub>H<sub>34</sub>O<sub>2</sub>), and stearamide (C<sub>18</sub>H<sub>37</sub>NO). The ESIMS of subfraction F-9 shows molecular ion peaks at *m/z* 281.246, establishing the molecular formula of linoleic acid (C<sub>18</sub>H<sub>32</sub>O<sub>2</sub>). The ESIMS of subfraction K-2 shows molecular ion peaks at *m/z* 123.0531, establishing the molecular formula of niacinamide (C<sub>6</sub>H<sub>6</sub>N<sub>2</sub>O) (Table 1). The chromatogram and mass spectrum peak list of the five isolated compounds can be found in the supplementary file. The remaining compounds with MFG scores above the cut-off values did not match any of the known molecules in the Metlin database, which leaves a large family of minor compounds in the PAEE still to be examined.

### Discussion

*P. australis* has been demonstrated to attenuate oxidative damage induced by high-dose corticosterone in PC-12 cells mimicking the effects of depression due to the presence of phytochemical compounds (16), indicating a protective role of *P. australis*-based anti-oxidants in the mitochondrial defense against ROS generation. Accumulating evidence indicates that suppression of microglia-mediated neuroinflammation is a potentially effective *therapeutic target* for halting the progression of neurodegenerative diseases (6, 33, 34).

In this study, we extended our investigation into the anti-neuroinflammatory potential of PAEE against LPS-stimulated neuroinflammation using BV2 microglial cells as the *in vitro* model system. We are particularly interested in elucidating the mechanism underlying the anti-inflammatory potential of PAEE by studying the expression of various proteins involved in inflammatory signaling pathways.

We observed that 1  $\mu$ g/ml LPS profoundly increased the production of NO and PGE<sub>2</sub> in BV2 microglial cells which is in line with previous findings (17, 28, 35-38). Conversely, pretreatment with 0.5-2.0 mg/ml PAEE significantly reduced the production of NO and PGE<sub>2</sub> in BV2 microglial cells. Notably, a study by Oh *et al.* (28) showed that *Sargassum serratifolium* ethanol extract at similar concentrations to that of PAEE (0.5 to 2.0  $\mu$ g/ml) also inhibited LPS-stimulated NO and PGE<sub>2</sub> production in BV2 microglial cells. Moreover, we found that the PAEE treatment demonstrated a higher

percentage of NO reduction compared with L-NAME, indicating PAEE is a potent inhibitor of NOS. A study by Gany *et al.* (17) observed that a low concentration of a *P. australis* dichloromethane or methanol extract (0.4 mg/ml) was able to inhibit NO production to  $73.63 \pm 3.81\%$  and  $75.67 \pm 0.21\%$ , respectively, which was similar to our finding that 0.5 mg/ml PAEE decreased NO production to 72.90%. Moreover, the *P. australis* methanol extract was found to inhibit PGE<sub>2</sub> production by 30%, which was 7% lower than that of 0.5 mg/ml PAEE at 37%.

Neuroinflammation and oxidative damage are undoubtedly hallmarks of neurodegeneration characterized by the generation and accumulation of excessive free radicals, including ROS and RNS, therefore contributing to disease progression (39, 40). Importantly, neuroinflammatory response has been shown to initiate cellular events associated with redox imbalance and microglia-derived oxidant production by NADPH oxidase. An excessive generation of intracellular and extracellular ROS leads to direct cellular damage and triggers the activation of microglia and leukocytes, which in turn, causes dysregulated generation of ROS and RNS, resulting in a vicious cycle. Indeed, ROS and RNS seem to be common features linked to microglial response, which is tightly related to Parkinson's disease (PD), Alzheimer's disease (AD), and frontotemporal dementia (FTD) involving dysfunctional protein aggregation and protein homeostasis imbalance. Considering the complex roles of oxidative damage in neuroinflammation, the regulation of cellular ROS may represent a potential treatment to impede neurodegeneration (37).

In this study, 1 µg/ml LPS increased intracellular ROS level, similar to the findings (36–38, 41). In contrast, pretreatment with PAEE markedly reduced ROS generation to 3.79- to 5.07-fold lower compared with LPS, indicating its protective effects against detrimental sequel of excessive accumulation of ROS by restoring redox balance via increased anti-oxidant activities (16). Overall, our results are very similar to those reported by Kim *et al.* (42) and others (43), who demonstrated ethanol extracts of various species of brown macroalgae including *Sargassum horneri*, *Saccharina japonica*, *Undaria pinnatifida*, *Sargassum fulvellum*, *Carpomitra costata* (42), and sargachromenol-enriched *Myagropsis myagroides* (43) had potent protective effects against neuroinflammation via suppressing ROS generation in BV2 microglial cells treated with LPS.

Consequently, NF-κB plays a key role in the regulation of microglia-mediated neuroinflammation. However, dysregulation of NF-κB has been linked to aberrant neuroinflammation through the release of pro-inflammatory mediators. Moreover, NF-κB-binding specific regions have been identified in pro-inflammatory genes such as iNOS, COX-2, TNF-α, and IL-6 (44). In particular, COX-2 triggers pro-inflammatory processes that can aggravate neuronal degeneration and functional impairments through PGE<sub>2</sub> production and subsequent activation of four G-protein coupled cell surface receptors, termed EP1, EP2, EP3, and EP4 receptors.

In this study, 1 µg/ml LPS increased the expression of iNOS and COX-2, which is similar to findings of other studies (36–38, 43). In contrast, pretreatment with PAEE significantly suppressed protein expressions of iNOS and COX-2, resulting in concomitant reductions of NO and PGE<sub>2</sub>. Ethanol extracts of other species of brown macroalgae, namely *M. myagroides* (42), *S. serratifolium* (28), and *C.*

*costata* (43) have also been demonstrated to decrease mRNA expression and protein levels of iNOS and COX-2, resulting in the inhibition of NO and PGE<sub>2</sub> production in BV2 microglial cells upon exposure to LPS.

We also observed that 1 µg/ml LPS increased the secretion of TNF-α and IL-6, similar to the findings of other studies (17, 37, 38, 45, 46). In contrast, pretreatment with 2.0 mg/ml PAEE exhibited the most potent activity by reversing the surge in TNF-α and IL-6 by 75.56% and 102.87%, respectively, suggesting its possible role in the attenuation of elevated level of circulating pro-inflammatory cytokines. On the other hand, Gany *et al.* (17) demonstrated that a low dose of *P. australis* methanol extract (0.4 mg/ml) attenuated  $94.45 \pm 1.92\%$  and  $92.07 \pm 1.99\%$  of TNF-α and IL-6, respectively. The discrepancy in these findings may be due to genetic variations or phenolic composition of *P. australis* from different geographical locations, extraction procedure, particle size, storage conditions and time, and the presence of interfering substances in the extracts (47). Likewise, ethanol extracts of *M. myagroides* (42) and *S. serratifolium* (28) have also been observed to decrease the protein level of TNF-α, IL-1β, and IL-6 in BV2 microglial cells upon exposure to LPS.

The LC-MS data revealed five compounds including esters, polyunsaturated fatty acids, and amides. Among these compounds, ethyl α-eleostearate, stearamide, linoleic acid, and niacinamide have been reported to possess therapeutic properties. Ethyl α-eleostearate or 9Z,11E,13E-octadecatrienoic acid ethyl ester is a conjugated PUFA derivative with anticancer properties. Yasui *et al.* (48) reported that ethyl α-eleostearate can reduce viability and induce apoptosis in human colon cancer CaCo-2 cells.

Stearamide derived from *Channa pleurophthalma* fin waste was found to possess anti-inflammation, antipruritic, antifungal, and antimicrobial properties using the Prediction of Activity Spectra for Substances (PASS) online tool (49). Another study (50) also reported that stearamide isolated from mushrooms such as *Amanita* sp., *Cantharellus* sp., *Ganoderma lucidum*, and *Lactarius kabansus* exhibited antibacterial properties against *Salmonella typhi*.

On the other hand, linoleic acid is an omega-6 (ω-6) polyunsaturated fatty acid (PUFA) that can be elongated and desaturated to form arachidonic acid, the precursor of various inflammatory cytokines (prostaglandins, leukotrienes, and endocannabinoids) (51). Collectively, ω-3 and ω-6 PUFAs, including linoleic acid, account for approximately 50% of the total lipids in red and brown macroalgae (52). Although preclinical evidence suggests that excess dietary linoleic acid increases the vulnerability to neuroinflammation (53), both ω-3 and ω-6 PUFAs have been shown to exhibit anti-inflammatory properties (54). In another study (55), pretreatment with linoleic acid for 24 hr reduced NO production and protein level of iNOS in BV2 microglial cells following exposure to LPS. Linoleic acid isolated from an ethyl acetate fraction of *Lignosus rhinocerotis* sclerotia has been found to suppress NO production and expression of iNOS and COX-2 in BV2 microglial cells (56). Moreover, researchers (57) observed that pretreatment with linoleic acid for 24 hr suppressed mRNA expression of COX-2 in BV2 microglial cells following exposure to Aβ<sub>42</sub> oligomers for 1 hr but not 4 hr, indicating the short-term protective effect of linoleic acid against neuroinflammation in an AD model.

In addition, niacinamide has been observed to inhibit



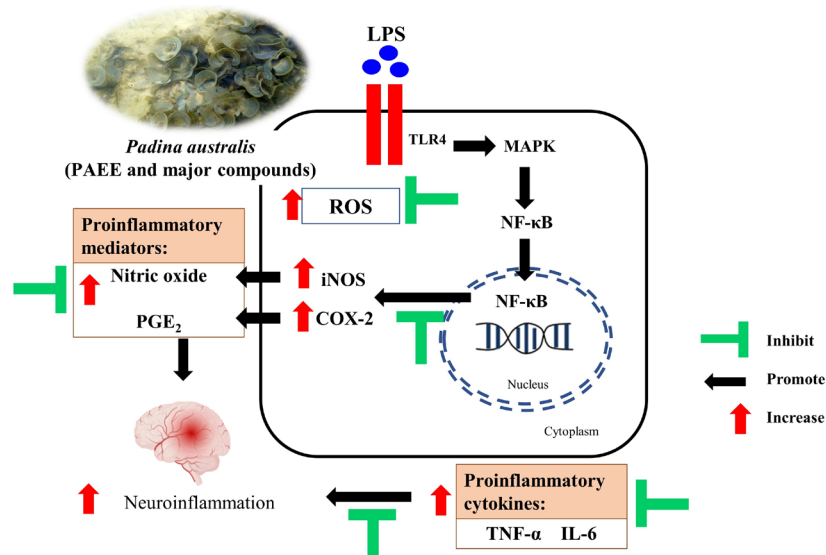


**Figure 8.** Proposed protective effects of PAEE against LPS-stimulated neuroinflammation in BV2 cells. Figure was created using BioRender (<https://biorender.com/>) and Microsoft PowerPoint 2017. The image of *P. australis* was captured at Cape Rachado, Port Dickson, Negeri Sembilan, Malaysia  
LPS: Lipopolysaccharide; PAEE: *Padina australis* ethanol extract

poly (ADP-ribose) polymerase 1 (PARP-1) that facilitates diverse inflammatory responses orchestrated by pro-inflammatory cytokines, chemokines, and adhesion molecules (58). The ability of niacinamide to pass rapidly and bi-directionally through the blood-brain barrier contributes to its efficacy in promoting neuroprotection (59). Furthermore, niacinamide has been found to ameliorate inflammation by reducing the mRNA expression of IL-1 $\beta$  and IL-6, and nuclear translocation of p-NF- $\kappa$ B in RAW264.7 macrophages (60). Overall, the anti-neuroinflammatory effects of *P. australis* were attributed to the presence of linoleic acid and niacinamide.

Taken together, our findings suggest that *P. australis* and its compounds possess protective effects against LPS-stimulated neuroinflammation in BV2 microglial cells. The proposed anti-neuroinflammatory mechanism of PAEE is presented in Figure 8, in which LPS interacts with TLR-4 leading to the activation of mitogen-activated protein kinase (MAPK) and nuclear factor- $\kappa$ B (NF- $\kappa$ B) signaling pathways. In the nucleus, activated NF- $\kappa$ B promotes the transcription of NF- $\kappa$ B-dependent genes in the regulation of expression of iNOS and COX-2, generating NO and PGE<sub>2</sub>, respectively. Upon exposure to 1  $\mu$ g/ml LPS, the anti-oxidant substances (16) and major compound of PAEE attenuated excessive generation of intracellular ROS, pro-inflammatory mediators (NO, PGE<sub>2</sub>, iNOS, and COX-2), and pro-inflammatory cytokines (TNF- $\alpha$  and IL-6). Taken together, our findings suggest that *P. australis* and its potential compounds possessed protective effects against LPS-stimulated neuroinflammation in BV2 microglial cells.

## Conclusion

Our current study demonstrated PAEE has protective effects against LPS-stimulated neuroinflammation in BV2 microglial cells by suppressing the excessive generation of intracellular ROS, and pro-inflammatory mediators and cytokines. These effects can be attributed to major compounds such as linoleic acid and niacinamide. The anti-neuroinflammatory and anti-oxidant properties of *P. australis* may lead to the development of novel therapeutic

strategies for neurodegenerative diseases.

## Acknowledgment

This research was financially supported by the University of Malaya Faculty of Medicine Research Grant (GPF003C-2019) and Sunway University Internal Grant (INT-2019-SST-DBS-04). We would like to thank the Public Service Department Malaysia and the Ministry of Health Malaysia for Full-Paid Leave (CBBP) with Federal Training Prize (HLP) [KKM500-7/92/730525085970(LDP 1) (6)] awarded to Kogilavani Subermaniam. The results presented in this paper were part of Kogilavani Subermaniam's thesis.

## Authors' Contributions

KS and KHW conceived the study; KS and SYL prepared the original draft; YYY, SHL, WSY, LWL, and KHW reviewed and edited the manuscript; KS, SYL, and LWL helped with visualization and illustration; YYY, SHL, and KHW supervised the study. All authors have agreed to the contents and approved the final version for publication.

## Conflicts of Interest

None.

## References

1. Yamanaka G, Suzuki S, Morishita N, Takeshita M, Kanou K, Takamatsu T, et al. Role of neuroinflammation and blood-brain barrier permeability on migraine. *Int J Mol Sci* 2021; 22: 8929.
2. Ginhoux F, Greter M, Leboeuf M, Nandi S, See P, Gokhan S, et al. Fate mapping analysis reveals that adult microglia derive from primitive macrophages. *Science* 2010; 330: 841-845.
3. Paolicelli RC, Bolasco G, Pagani F, Maggi L, Scianni M, Panzanelli P, et al. Synaptic pruning by microglia is necessary for normal brain development. *Science* 2011; 333: 1456-1458.
4. Simpson D, Oliver PL. ROS generation in microglia: Understanding oxidative stress and inflammation in neurodegenerative disease. *Anti-oxidants (Basel)* 2020; 9: 743.
5. Zhang P, Yang M, Chen C, Liu L, Wei X, Zeng S. Toll-like receptor 4 (TLR4)/opioid receptor pathway crosstalk and impact

- on opioid analgesia, immune function, and gastrointestinal motility. *Front Immunol* 2020; 11: 1455.
6. Seow SL, Naidu M, Sabaratnam V, Vidyadaran S, Wong KH. Tiger's Milk medicinal mushroom, *Lignosus rhinocerotis* (Agaricomycetes) sclerotium inhibits nitric oxide production in LPS-stimulated BV2 microglia. *Int J Med Mushrooms* 2017; 19: 405-418.
  7. Pang JR, Goh VMJ, Tan CY, Phang SM, Wong KH, Yow YY. Neuritogenic and *in vitro* anti-oxidant activities of Malaysian *Gracilaria manilaensis* Yamamoto & Trono. *J Appl Phycol* 2018; 30: 3253-3260.
  8. Pang JR, How SW, Wong KH, Lim SH, Phang SM, Yow YY. Cholinesterase inhibitory activities of neuroprotective fraction derived from red alga *Gracilaria manilaensis*. *Fish Aquatic Sci* 2022; 25: 49-63.
  9. Ngu EL, Ko CL, Tan CY, Wong KH, Phang SM, Yow YY. Phytochemical profiling and *in vitro* screening for neuritogenic and anti-oxidant activities of *Spirulina platensis*. *Indian J Pharm Educ Res* 2021; 55: 812-822.
  10. Subermaniam K, Teoh SL, Yow YY, Tang YQ, Lim LW, Wong KH. Marine algae as emerging therapeutic alternatives for depression: A review. *Iran J Basic Med Sci* 2021; 24: 997.
  11. Yow YY, Goh TK, Nyiew KY, Lim LW, Phang SM, Lim SH, et al. Therapeutic potential of complementary and alternative medicines in peripheral nerve regeneration: A systematic review. *Cells* 2021; 10: 2194.
  12. Bruno JF, Bertness MD. Habitat modification and facilitation in benthic marine communities. In: Bertness MD, Gaines SD, Hay ME, editors. *Marine Community Ecology*. Sinauer Associates; 2001.p. 201-218.
  13. Schiel DR, Foster MS. The population biology of large brown seaweeds: Ecological consequences of multiphase life histories in dynamic coastal environments. *Annu Rev Ecol Evol Syst* 2006; 37: 343-372.
  14. Mineur F, Arenas F, Assis J, Davies AJ, Engelen AH, Fernandes F, et al. European seaweeds under pressure: Consequences for communities and ecosystem functioning. *J Sea Res* 2015; 98: 91-108.
  15. Teagle H, Hawkins SJ, Moore PJ, Smale DA. The role of kelp species as biogenic habitat formers in coastal marine ecosystems. *J Exp Mar Biol Ecol* 2017; 492: 81-98.
  16. Subermaniam K, Yow YY, Lim SH, Koh OH, Wong KH. Malaysian macroalga *Padina australis* Hauck attenuates high dose corticosterone-mediated oxidative damage in PC12 cells mimicking the effects of depression. *Saudi J Biol Sci* 2020; 27: 1435-1445.
  17. Gany SA, Tan SC, Gan SY. Anti-oxidative, anticholinesterase and anti-neuroinflammatory properties of Malaysian brown and green seaweeds. *Int J Ind Syst Eng* 2014; 8: 1269-1275.
  18. Murugan AC, Vallal D, Karim MR, Govidan N, Yusoff MBM, Rahman MM. *In vitro* antiradical and neuroprotective activity of polyphenolic extract from marine algae *Padina australis*. *J Chem Pharm Res* 2015; 7: 355-362.
  19. Akbary P, Aminikhoei Z, Hobbi M, Samadi Kuchaksaraei B, Rezaei Tavabe K. Anti-oxidant properties and total phenolic contents of extracts from three macroalgae collected from Chabahar coasts. *Proc Natl Acad Sci U S A* 2021; 91: 327-334.
  20. Chong C-W, Hii S-L, Wong C-L. Antibacterial activity of *Sargassum polycystum* C. Agardh and *Padina australis* Hauck (phaeophyceae). *Afr J Biotechnol* 2011; 10: 14125-14131.
  21. Zailanie K. Study of *Padina australis* using UV-VIS, HPLC and antibacterial. *J Life Sci Biomed* 2016; 6: 01-05.
  22. Jaswir I, Noviendri D, Salleh HM, Taher M, Miyashita K. Isolation of fucoxanthin and fatty acids analysis of *Padina australis* and cytotoxic effect of fucoxanthin on human lung cancer (H1299) cell lines. *Afr J Biotechnol* 2011; 10: 18855-18862.
  23. Wang H, Ooi EV, Ang PO Jr. Antiviral activities of extracts from Hong Kong seaweeds. *J Zhejiang Univ Sci B* 2008; 9: 969-976.
  24. Canoy JL, Bitacura JG. Cytotoxicity and antiangiogenic activity of *Turbinaria ornata* Agardh and *Padina australis* Hauck ethanolic extracts. *Anal Cell Pathol (Amst)* 2018; 2018: 3709491.
  25. Tirtawijaya G, Mohibullah M, Meinita MDN, Moon IS, Hong YK. The ethanol extract of the rhodophyte *Kappaphycus alvarezii* promotes neurite outgrowth in hippocampal neurons. *J Appl Phycol* 2016; 28: 2515-2522.
  26. Trono GC Jr. *Field Guide and Atlas of the Seaweed Resources of the Philippines*. Bookmark Inc.; 1997.
  27. Harun A, Vidyadaran S, Lim SM, Cole AL, Ramasamy K. Malaysian endophytic fungal extracts-induced anti-inflammation in lipopolysaccharide-activated BV-2 microglia is associated with attenuation of NO production and, IL-6 and TNF- $\alpha$  expression. *BMC Complement Altern Med* 2015; 15: 166.
  28. Oh S-J, Joung E-J, Kwon M-S, Lee B, Utsuki T, Oh C-W, et al. Anti-inflammatory effect of ethanol extract of *Sargassum serratifolium* in lipopolysaccharide-stimulate BV2 microglia. *J Med Food* 2016; 19: 1023-1031.
  29. Kim N, Yoo H-S, Ju Y-J, Oh MS, Lee K-T, Inn K-S, et al. Synthetic 3',4'-dihydroxyflavone exerts anti-neuroinflammatory effects in BV2 microglia and a mouse model. *Biomol Ther (Seoul)* 2018; 26: 210-217.
  30. Yap WF, Tay V, Tan SH, Yow YY, Chew J. Decoding anti-oxidant and antibacterial potentials of Malaysian green seaweeds: *Caulerpa racemosa* and *Caulerpa lentillifera*. *Antibiotics (Basel)* 2019; 8: 152.
  31. Bertin MJ, Zimba PV, Beauchesne KR, Huncik KM, Moeller PDR. Identification of toxic fatty acid amides isolated from the harmful alga *Prymnesium parvum* Carter. *Harmful Algae* 2012; 20: 111-116.
  32. Song SB, Park JS, Chung GJ, Lee IH, Hwang ES. Diverse therapeutic efficacies and more diverse mechanisms of nicotinamide. *Metabolomics* 2019; 15: 137.
  33. Cai Y, Liu J, Wang B, Sun M, Yang H. Microglia in the neuroinflammatory pathogenesis of Alzheimer's disease and related therapeutic targets. *Front Immunol* 2022; 13: 856376.
  34. Bachiller S, Jiménez-Ferrer I, Paulus A, Yang Y, Swanberg M, Deierborg T, et al. Microglia in neurological diseases: A road map to brain-disease dependent-inflammatory response. *Front Cell Neurosci* 2018; 12: 488.
  35. Jayasooriya R, Moon D, Choi YH, Yoon CH, Kim GY. Methanol extract of *Hydroclathrus clathratus* inhibits production of nitric oxide, prostaglandin E<sub>2</sub> and tumor necrosis factor- $\alpha$  in lipopolysaccharide-stimulated BV2 microglial cells via inhibition of NF- $\kappa$ B activity. *Trop J Pharm Res* 2011; 10: 723-730.
  36. Jayasooriya RGPT, Lee K-T, Choi YH, Moon S-K, Kim W-J, Kim G-Y. Antagonistic effects of acetylshikonin on LPS-induced NO and PGE<sub>2</sub> production in BV2 microglial cells via inhibition of ROS/PI3K/Akt-mediated NF- $\kappa$ B signaling and activation of Nrf2-dependent HO-1. *In Vitro Cell Dev Biol Anim* 2015; 51: 975-986.
  37. Chan C-K, Tan LT-H, Andy SN, Kamarudin MNA, Goh B-H, Abdul Kadir H. Anti-neuroinflammatory activity of *Elephantopus scaber* L. via activation of Nrf2/HO-1 signaling and inhibition of p38 MAPK pathway in LPS-induced microglia BV-2 cells. *Front Pharmacol* 2017; 8: 397.
  38. Zang C, Yang H, Wang L, Wang Y, Bao X, Wang X, et al. A novel synthetic derivative of phloroglucinol inhibits neuroinflammatory responses through attenuating kalirin signaling pathway in murine BV2 microglial cells. *Mol Neurobiol* 2019; 56: 2870-2888.
  39. Fischer R, Maier O. Interrelation of oxidative stress and inflammation in neurodegenerative disease: Role of TNF. *Oxid Med Cell Longev* 2015; 2015: 610813.
  40. Troubat R, Barone P, Leman S, Desmidt T, Cressant A, Atanasova B, et al. Neuroinflammation and depression: A review. *Eur J Neurosci* 2021; 53: 151-171.
  41. Velagapudi R, El-Bakoush A, Lepiarz I, Ogunrinade F, Olajide

- OA. AMPK and SIRT1 activation contribute to inhibition of neuroinflammation by thymoquinone in BV2 microglia. *Mol Cell Biochem* 2017; 435: 149-162.
42. Kim S, Lee M-S, Lee B, Gwon W-G, Joung E-J, Yoon N-Y, et al. Anti-inflammatory effects of sargachromenol-rich ethanol extract of *Myagropsis myagroides* on lipopolysaccharide-stimulated BV-2 cells. *BMC Complement Altern Med* 2014; 14: 231.
43. Park C, Cha HJ, Hong SH, Kim S, Kim HS, Choi YH. *Carpomitra costata* extract alleviates lipopolysaccharide-induced neuroinflammatory responses in BV2 microglia through the inactivation of NF- $\kappa$ B associated with the blockade of the TLR4 pathway and ROS generation. *Hanguk Haeyang Paio Hakhoe* 2020; 12: 29-39.
44. Liu T, Zhang L, Joo D, Sun SC. NF- $\kappa$ B signaling in inflammation. *Signal Transduct Target Ther* 2017; 2: 17023.
45. Wang H, Vidyadaran S, Mohd Moklas MA, Baharuldin MTH. Inhibitory activity of *Ficus deltoidea* var. *trengganuensis* aqueous extract on lipopolysaccharide-induced TNF- $\alpha$  production from microglia. *Evid Based Complement Alternat Med* 2017; 2017: 2623163.
46. Wong CH, Gan SY, Tan SC, Gany SA, Ying T, Gray AI, et al. Fucosterol inhibits the cholinesterase activities and reduces the release of pro-inflammatory mediators in lipopolysaccharide and amyloid-induced microglial cells. *J Appl Phycol* 2018; 30: 3261-3270.
47. Mekinić IG, Skroza D, Šimat V, Hamed I, Čagalj M, Popović Perković Z. Phenolic content of brown algae (Pheophyceae) species: Extraction, identification, and quantification. *Biomolecules* 2019; 9: 244.
48. Yasui Y, Hosokawa M, Sahara T, Suzuki R, Ohgiya S, Kohno H, et al. Bitter melon seed fatty acid rich in 9c,11t,13t-conjugated linolenic acid induces apoptosis and up-regulates the GADD45, p53 and PPAR $\gamma$  in human colon cancer Caco-2 cells. *Prostaglandins Leukot Essent Fatty Acids* 2005; 73: 113-119.
49. Riyadi PH. The effectivity of Kerandang fish (*Channa pleurophthalma* Blkr) fin waste as an anti-skin allergies agent. *Syst Rev Pharm* 2020; 11: 26-31.
50. Reid T, Kashangura C, Chidewe C, Benhura MA, Stray-Pedersen B, Mduluza T. Characterization of anti-*Salmonella typhi* compounds from medicinal mushroom extracts from Zimbabwe. *Int J Med Mushrooms* 2019; 21: 713-724.
51. Ramsden CE, Ringel A, Feldstein AE, Taha AY, MacIntosh BA, Hibbeln JR, et al. Lowering dietary linoleic acid reduces bioactive oxidized linoleic acid metabolites in humans. *Prostaglandins Leukot Essent Fatty Acids* 2012; 87: 135-141.
52. Pradhan B, Nayak R, Patra S, Jit BP, Ragusa A, Jena M. Bioactive metabolites from marine algae as potent pharmacophores against oxidative stress-associated diseases: A comprehensive review. *Molecules* 2021; 26: 37.
53. Taha AY. Linoleic acid-good or bad for the brain? *NPJ Sci Food* 2020; 4: 1.
54. Navarro-Xavier RA, de Barros KV, de Andrade IS, Palomino Z, Casarini DE, Flor Silveira VL. Protective effect of soybean oil- or fish oil-rich diets on allergic airway inflammation. *J Inflamm Res* 2016; 9: 79-89.
55. Lowry JR, Marshall N, Wenzel TJ, Murray TE, Klegeris A. The dietary fatty acids  $\alpha$ -linolenic acid (ALA) and linoleic acid (LA) selectively inhibit microglial nitric oxide production. *Mol Cell Neurosci* 2020; 109: 103569.
56. Nallathamby N, Serm LG, Raman J, Malek S, Vidyadaran S, Naidu M, et al. Identification and *in vitro* evaluation of lipids from sclerotia of *Lignosus rhinocerotis* for anti-oxidant and anti-neuroinflammatory activities. *Nat Prod Commun* 2016; 11: 1485-1490.
57. Ma QL, Zhu C, Morselli M, Su T, Pelligrini M, Lu Z, et al. The novel omega-6 fatty acid docosapentaenoic acid positively modulates brain innate immune response for resolving neuroinflammation at early and late stages of humanized APOE-based Alzheimer's disease models. *Front Immunol* 2020; 11: 558036.
58. Salech F, Ponce DP, Paula-Lima AC, SanMartin CD, Behrens MI. Nicotinamide, a poly [ADP-ribose] polymerase 1 (PARP-1) inhibitor, as an adjunctive therapy for the treatment of Alzheimer's disease. *Front Aging Neurosci* 2020; 12: 255.
59. Spector R. Niacinamide transport through the blood-brain barrier. *Neurochem Res* 1987; 12: 27-31.
60. Giri B, Belanger K, Seamon M, Bradley E, Purohit S, Chong R, et al. Niacin ameliorates neuro-inflammation in Parkinson's disease via GPR109A. *Int J Mol Sci* 2019; 20: 4559.